Physica A 440 (2015) 185–199

Contents lists available at ScienceDirect

Physica A

journal homepage: www.elsevier.com/locate/physa

An entropical characterization for complex systems becoming out of control

Marcos E. Gaudiano *

GRSI-FCEFyN, Universidad Nacional de Córdoba, Ciudad Universitaria CP 5000, Córdoba, Argentina
CIEM-CONICET, Ciudad Universitaria CP 5000, Córdoba, Argentina
ATP-group, CMAF, Instituto para a Investigação Interdisciplinar, P-1649-003 Lisboa Codex, Portugal

HIGHLIGHTS

- We study complex systems whose components have a hierarchical sub-structure.
- The system is partitioned into cells to which a generalized entropy S is associated.
- The different regimes of S define an entropical classification of the components.
- This classification is independent of the observer's criteria.
- The normalized S can be associated to an evolution in the absence of control.

ARTICLE INFO

Article history:
Received 8 April 2015
Received in revised form 1 August 2015
Available online 24 August 2015

Keywords:
Fractal
Entropy
Complex systems
Structures and organization

ABSTRACT

General properties of N-dimensional multi-component or many-particle systems exhibiting self-similar hierarchical structure are presented. The entire system is partitioned into cells, which have an associated generalized entropy $S(D)$ that is shown to be a universal function of the fractal dimension D of the configurations, exhibiting self-similarity properties which are independent of the dimensionality N. This provides a general way to classify the components of the system according to entropical reasons, independently of the observer's criteria. For certain complex systems, the normalized $S(D)$ may also be associated with the large time stationary profile of the fractal density distribution in the absence of external fields (or control).

1. Introduction

Multi-component, strongly correlated systems, often exhibit non-linear behavior at the microscale leading to emergent phenomena at the macroscale. As P.W. Anderson stated back in 1972, it often happens that *"the whole becomes not only more but very different from the sum of its parts"* [1]. Fingerprints of such emergent phenomena can be identified in hierarchical behavior [2,3] or constraints [4,5], sometimes associated with fractal behavior [6].

Hierarchical behavior exhibiting self-similarity has been identified in physical, social, biological and technological systems [7]. Employing theoretical tools, such as the *singularity spectrum* or its equivalent, *multiscaling exponents* (via a Legendre's transformation), etc., fractal analysis has been applied to geophysics, medical imaging, market analysis, voice recognition, solid state physics, etc. (see e.g. Refs. [8–12]). Recently, high quality spatio-temporal fractal behavior in connection with built-up areas in planar embeddings [13] has been unraveled, whose diversity of fractal dimensions covered

* Correspondence to: GRSI-FCEFyN, Universidad Nacional de Córdoba, Ciudad Universitaria CP 5000, Córdoba, Argentina.
E-mail address: marcosgaudiano@gmail.com.

http://dx.doi.org/10.1016/j.physa.2015.08.023
0378-4371/

the entire [0, 2] dimensionality spectrum, reflecting the presence of self-organizing principles which strongly constrain the spatial layout of the urban landscape. Nevertheless, the ideas developed in Ref. [13] are by no means restricted to the study of Urban Dynamics. This is the starting point of the present work, which introduces a general framework to describe the behavior of multi-component complex systems constrained to exhibit fractal behavior in a space of arbitrary dimensionality N. New properties, ideas and concepts applicable to the study of Complex Systems arise from this generalization, which will be developed as follows.

Section 2 outlines the classes of complex systems studied, the hierarchies associated to its components, and the central role that the concept of entropy will play in this article. Section 3 shows many estimates that enable us to numerically analyze and compute the entropy function for $N > 2$. Section 4 introduces self-similar properties that are used to carry out a pattern analysis of the components. All the ideas developed in the previous sections will be finally applied to study Complex Systems evolving *in the absence of control* in Section 5.

2. Classes of complex systems studied and entropy function

2.1

It is assumed that the complex systems of this article will be constituted of many interacting components. Every component will have a kind of hierarchical internal sub-structure [14], whose associated hierarchy will be indexed by some number D, ranging between a pair of minimum and maximum values, say $D = 0$ and $D = N > 0$, respectively. Thus, the hierarchies will be ordered and the components of the system could be classified according to D. Even for many systems, the hierarchy D may not only indicate something about the structure of the component, but it could also define a specific type of dynamics (or *pattern* of behavior) that the component follows, as it interacts with the rest.

Physics often needs to define ideal models ranging from say, *spherical horses in vacuum* [15] to symplectic structures of dynamical laws of any kind (relativistic, Newtonian, quantum, etc.). Clearly, all these structures cannot be applied to complex systems. In contrast, the systems of this nature seem to follow so complex dynamical laws that a good idea could be – perhaps – setting our point of reference at the opposite side, i.e. at a kind of *worst possible ideal scenario*, which will be out-of-control, in the sense that our knowledge about what is inside each component is minimal. This scenario may be represented by a distribution function $\rho_*(D)$,[1] so that the number of components with hierarchy index D will be proportional to our ignorance of the particular dynamics represented by D. Given that the physical notion of entropy corresponds to a measure of how much one does not know about something, we shall assume that $\rho_*(D)$ is given by:

$$\rho_*(D) = \frac{S(D)}{\int_0^N S(x)\,\mathrm{d}x,} \tag{1}$$

where $S(D)$ is an entropy function in a generalized sense. Of course, how one could precisely define a hierarchy index D and its entropy function $S(D)$ for a general complex system, is a difficult question to answer. An alternative to this can be found in the article [13].

The article is about Urban Dynamics and Complexity. In it, a metropolitan area is visualized as composed of many cells (squares of 1 km side), each one indexed by a *number* associated to the way the structure of the built-up area inside of it is hierarchically organized. The *number* is the fractal dimension D of the built-up area of the cell. Similarly, throughout the present article, it will be assumed that the fractal dimension D indexes the hierarchies and their associated dynamics of the components. This is just one of the reasons why the letter D was chosen at the beginning of this section.

The second reason has to do with Fig. 1, which was not included in Ref. [13]. Every red curve corresponds to the plot of an entropy function $S(D)$ defined (in Refs. [13]) as the log-number of the possible cell built-up area configurations, having fractal dimension equal to D. The successive proximity of the distribution of cells $\rho(D)$ to $\rho_*(D) = S(D)/\int_0^2 S(x)\,\mathrm{d}x$ ($N = 2$, see Eq. (1)) is a subtle fact that is worth mentioning. The city under consideration in the article is Lisbon, for which there is a well-documented urban sprawl together with a number of urbanistic problems, due to either weak regulations or vague governmental controls in urban planning (see also Ref. [16]) during a period of more than 40 years. Clearly, *urban sprawl* is an out-of-control situation and I suggest that Fig. 1 could be seen as a *signature* of this, due to the notion that what cannot be controlled is precisely what is ignored. Then, given that $S(D)$ measures ignorance, it could be interpreted as proportional to the maximum degree of uncontrollability of the cells having dimension D. Thus, $\rho_*(D)$ represents the ideal worst possible scenario mentioned above, in which the amount of cells of some type D is proportional to how much out of control they can be. In connection with the title of the present work, we will get back to this issue in Section 5.

2.2

First of all, it is important to understand why the characterization presented in Ref. [13] in terms of counting the number of cell fractal configurations, is an idea very plausible to apply to many other higher dimensional complex systems, having – in principle – nothing to do with Urban Dynamics.

[1] I.e. satisfying $\int_0^N \rho_*(D)\,\mathrm{d}D = 1$ and such that $\rho_*(D)\mathrm{d}D$ is the fraction of components with a hierarchy index equal to D.

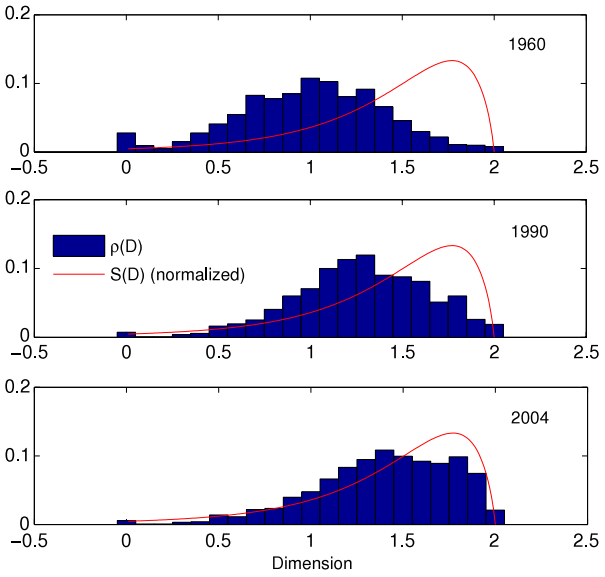

Fig. 1. The distribution $\rho(D)$ of fractal dimensions of Lisbon for the years 1960, 1990 and 2004. In this article, a connection between the well-documented urban sprawl of the city and the successive proximity of $\rho(D)$ to the normalized entropy function $S(D)$ is suggested. (For interpretation of the references to color in this figure legend, the reader is referred to the web version of this article.)

It will prove convenient to represent our multi-component system in terms of *black* pixels (each one a hypercube of side 1) embedded in a space of dimensionality N otherwise filled with *white* pixels. Let us assume the entire system is divided into a grid of cells (bigger hypercubes) of side λ (see Appendix D), to each of which the standard box-counting method (*BCM*) is applied in order to assess the (local[2]) fractal dimension D of the part of the system lying on it [19].

For each cell, the total number of possible configurations is 2^{λ^N}. The volume V of the pixels in each cell that belong to the system can in principle vary between 0 and λ^N. However, if the system exhibits a local fractal dimension D, the number of system configurations is strongly reduced, and it will also depend on the fraction of the cell volume occupied by the system. This conforms with the notion that an emerging property of a complex system provides a constraining condition regarding its "entropy" (in a generalized sense), viewed here as the log-number of possible configurations of the system compatible with the specified value of the emergent macroscopic variable [20]. Before dwelling on the problem of the number of configurations, we shall start by determining lower $L(D)$ and upper $U(D)$ bounds for the volume of a given cell compatible with a pre-defined fractal dimension D.

According to the *BCM*, there exists a minimal number N_k of hyper-boxes of side 2^k ($k = 0, 1, 2, \ldots$) that cover the pixels of the system inside the cell, which approximately satisfies:

$$\log N_k = -Dk + B \tag{2}$$

(throughout this article, "log" will be used as a shorthand for "$\log_2$") where D is the fractal dimension and B is a constant which is not associated to the fractal behavior [6].

Clearly, since this article is an attempt to represent real-world systems, the number of scales involved in the fractal behavior will always be finite. Thus, we will assume that Eq. (2) holds for $k = 0, \ldots, m$, with

$$m = [\log(\lambda/2)]. \tag{3}$$

The constant B just shifts the linear fitting up or down, according to the multiple values that V can have. Taking $k = 0$ in Eq. (2) one has that $\log N_0 = B$, where N_0 is the number of pixels that belong to the system, i.e. its volume V; thus, $B = \log V$.

Hence, in particular we have that $\log V = Dm + \log N_m$. On the other hand, N_m is just the number of boxes of edge 2^m: $1 \leq N_m \leq (\lambda/2^m)^N$. Put together, we obtain,

$$L(D) \doteq 2^{mD} \leq V \leq \lambda^N (2^m)^{D-N} \doteq U(D). \tag{4}$$

Thus, there is no configuration with fractal dimension D and with a volume V outside of the bounded region defined by Eq. (4) (Fig. 1 of Ref. [13] and Fig. 4 of Ref. [17] are examples of this, for $N = 2$). It is quite remarkable that the lower bound

[2] As in the particular fractal system studied in Ref. [13], the general systems studied in this article are assumed to be (in part) randomly generated and having a fractal dimension that depends on the position (like many other real-world complex systems: deforested areas [17], 3D cancerous tissues [18] or any other multi-dimensional imaginable complex system). Thus, these systems have nothing to do with the classical mathematical fractals that can be found in the literature (like Cantor's set, Sierpinski's carpet, etc.) to which it is possible to assign a (single) fractal dimension.

$L(D)$ is independent of the embedding dimension N. Knowledge of these constraints on the cell volume compatible with a given fractal dimension D considerably simplifies the determination of the total number of configurations accessible to the system in a cell exhibiting a fractal dimension D. Let us denote this quantity by $\Omega(V, D)$, where V is the volume occupied by the system in the cell.

From Eq. (2), taking $B = \log V$, the number of boxes covering the part of the system inside the cell at the kth stage of the *BCM* satisfies $N_k = N_{k-1}2^{-D}$. N_k is thus defined by V and D, but does not depend on the final configuration. In addition, the previous equation defines a recursive sequence in which each of the N_k boxes is sub-divided into 2^N sub-boxes; of them, N_{k-1} will be picked up to enclose the system at the previous $k-1$th stage. The number of ways this procedure can be done is equal to $f(2^N, N_k, N_{k-1})$ (see Appendix A), leading to

$$\Omega(V, D) = \prod_{k=1}^{m} f(2^N, V2^{-kD}, 2^D V2^{-kD}) \tag{5}$$

whereas the total number of configurations having dimension D is given by:

$$\Omega(D) = \sum_{V=L(D)}^{U(D)} \Omega(V, D). \tag{6}$$

For a given cell of the grid, the function

$$S(D) = \log \Omega(D) \tag{7}$$

defines a generalized entropy compatible with a cell dimension equal to D.

3. Estimates of $S(D)$

This section is about the computation of many estimates of $S(D)$, which will enable the analysis of this quantity for $N > 2$, the visualization of the usual orders of magnitude involved with it, as well as the study of the robustness of its definition in terms of the coarse-graining level. All these estimates turn out to be very important for the ideas discussed in the following two sections.

3.1

In order to study the general properties of $S(D)$ for spaces of arbitrary dimensionality N, Eq. (7) must be computed accurately. Function f plays an important role in the definition of $S(D)$ (Eqs. (5) and (7)). f can be generalized in a straightforward way (from the case $N = 2$ of Ref. [13]), as it is shown in Appendix A. However, its numerical evaluation takes too much time just for $N = 3$, increasing doubts about its precision and becoming an impossible task for higher N. The reason is that $\Omega(D)$ is a huge number. For instance, just for $N = 2$ and $\lambda = 100$ ($m = 5$ steps in the *BCM*), it turns out that $\max_D \Omega(D) \sim 10^{1300}$. A way to avoid these difficulties is to find a good approximation of f that, at the same time, should be easier to evaluate. Actually, in Appendix B.2 it is shown that

$$\log f(x, y, z) \approx \log \binom{xy}{z} \tag{8}$$

if y and z are large numbers, which is all what we need, as it is explained below.

For simplicity, we shall use $U = U(D)$ and $L = L(D)$, except where explicitly indicated. From (5), (6) one has that:

$$S(D) \geq \log f(2^N, U2^{-D}, U) \approx \log \binom{2^{N-D}U}{U}$$

because U is the largest possible volume V, so we can use Eq. (8). This indicates that

$$S(D) \gtrsim \log(2^{N-D})^U = \lambda^N (2^m)^{D-N}(N - D), \tag{9}$$

then, maximizing:

$$\max_D S(D) \gtrsim \frac{\lambda^N}{e \ln 2^m} \geq \frac{\lambda^N}{e \ln \frac{\lambda}{2}}, \tag{10}$$

i.e. the maximum of $S(D)$ grows *exponentially* with N. In contrast, the local minima of $S(D)$ at $D = 0$ and $D = N$ will usually be very small in comparison with the maximum. For instance, due to $f(x, y, y) = x^y$ (see Appendix A), for $D = 0$ one has from Eqs. (4) and (6) that

$$S(0) = \log \left(\sum_{V=1}^{(\lambda/2^m)^N} 2^{mNV} \right) \approx \frac{mN}{2^{mN}} \lambda^N \ll \lambda^N \sim \max_D S(D), \tag{11}$$

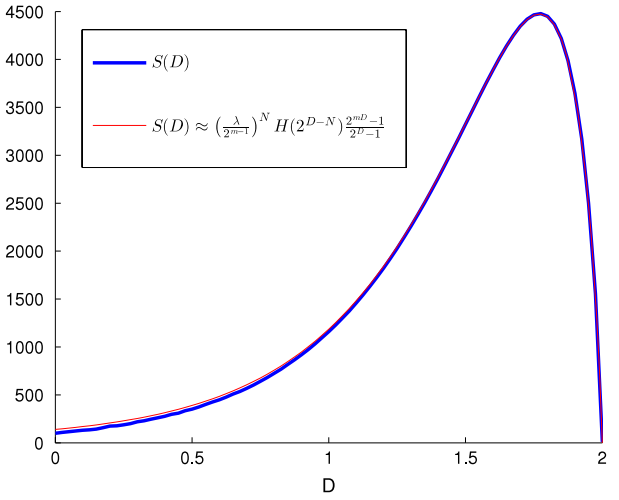

Fig. 2. Comparison between $S(D)$ defined by Eq. (7) and its estimate given by Eq. (18), for the case $N = 2$ and $\lambda = 100$.

for reasonable N and m. Similarly, because $f(x, y, xy) = 1$ (see Appendix A), for $D = N$ one has that $S(N) = \log(U(N) - L(N) + 1) = \log(\lambda^N - 2^{mN} + 1) > 0$ (Eq. (3)), independently of N. Then, given that $L \geq 1$ one has that

$$S(N) \leq N \log \lambda \ll \lambda^N \sim \max_D S(D). \tag{12}$$

On the other hand, as usual, replacing $\Omega(D)$ by the largest of $\Omega(V, D)$ constitutes a good approximation. Indeed, Eq. (B.1) implies that given D, $f(2^N, 2^N V/2^{kD}, 2^D V/2^{kD})$ is an increasing function of V ($k = 0, \ldots, m$) as well as $\Omega(V, D)$ (see Eq. (5)); hence, from Eqs. (5) and (6), one has that:

$$S(D) \leq \log(U - L + 1) + \log \Omega(U, D). \tag{13}$$

Then, given that $L \geq 1$:

$$0 \leq S(D) - \log \Omega(U, D) \leq \log U \leq N \log \lambda \tag{14}$$

(see Eq. (4)). In other words, the upper bound of Eq. (14) matches the value of the estimate of the local minimum of $S(D)$ at $D = N$ (Eq. (12)). Thus, Eq. (14) provides a good estimate for $S(D)$, by just assuming the summation in (6) to be approximately equal to its greatest summand $\Omega(U, D)$, i.e.:

$$S(D) \approx \log \Omega(U, D). \tag{15}$$

Now, according to Eq. (5), the above formula becomes:

$$S(D) \approx \sum_{k=1}^{m} \log f(2^N, U2^{-kD}, 2^D U2^{-kD}) \approx \sum_{k=1}^{m} \log \binom{2^N U2^{-kD}}{2^D U2^{-kD}} \tag{16}$$

because of the fact that every 2nd and 3rd arguments at which f is evaluated are large numbers (i.e. $V = U$, so we can use Eq. (8) again).

Stirling's approximation $\log \binom{x}{y} \approx xH(y/x)$ works well if x and y are large, where

$$H(t) = -t \log t - (1 - t) \log(1 - t) \tag{17}$$

is the Shannon's binary entropy function. This useful relationship can be applied to Eq. (16), arriving at an explicit, easy-to-analyze and excellent approximation of the formula of $S(D)$ (see Fig. 2):

$$S(D) \approx \left(\frac{\lambda}{2^{m-1}}\right)^N H(2^{D-N}) \frac{2^{mD} - 1}{2^D - 1}. \tag{18}$$

3.2

Let us analyze the robustness of the definition of $S(D)$, an important point that was not studied in Ref. [13]. Actually, for another length $\bar{\lambda}$ of the side of the boxes of the grid, that does not differ in orders of magnitude with λ (that is, if m remains

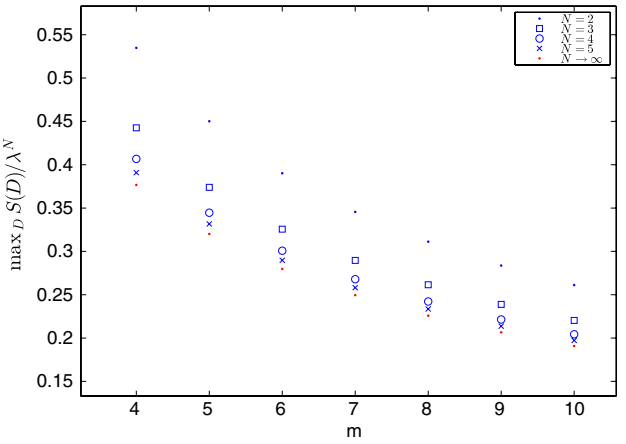

Fig. 3. Plot of $\max_D S(D)/\lambda^N$ for $m = 4, \ldots, 10$ and $N = 2, \ldots, 10$.

invariant, see Eq. (3)), one can similarly define the number of configurations as well as the associated entropy, say $\bar{\Omega}(D)$ and $\bar{S}(D)$, respectively. Whatever be the case, from Eq. (18) we have that

$$S(D) \approx (\lambda/\bar{\lambda})^N \bar{S}(D) \tag{19}$$

so, $S(D)$ and $\bar{S}(D)$ will be approximately proportional to each other[3]; consequently, it is possible to conclude the definition of $S(D)$ is *robust to the choice of* λ because the shape of this function is independent of that parameter.

4. Pattern analysis

This section describes a general classification of patterns based on entropical reasons which, consequently, does not depend on the observer's criteria. First, in connection with this, it is worth inquiring into the total number of patterns that we are talking about.

4.1

The fractal behavior assumed here, together with the existence of a coarse-graining scale λ and its associated $S(D)$, strongly constrains the number of possible overall configurations the system cells may explore, dramatically reducing this number compared to an uncorrelated multi-component system. Let us illustrate these ideas, quantitatively. If our fractal analysis is carried out with a precision – in dimensionality – of δD, the total number of configurations of a given cell exhibiting a fractal behavior can be roughly bounded by:

$$\Omega_{total} \doteq \sum_{0 \le D \le N} \Omega(D) \le \frac{N}{\delta D} \max_D \Omega(D). \tag{20}$$

On the other hand, from Eq. (18), it is very easy to obtain (numerically) $\max_D S(D)$ (see Fig. 3). Clearly, the figure shows that $\max_D S(D)$ is always strictly less than λ^N. Thus, for a given cell, the number of fractal configurations will always be just a tiny fraction of the total number of possible, uncorrelated configurations, given by 2^{λ^N}. For example, it is easy to see from Fig. 3 and Eq. (7) that for $N = 2$ and $\lambda = 100$ ($m = 5$):

$$\Omega_{total} \lesssim \frac{10^{1300}}{\delta D}. \tag{21}$$

The right member of the previous equation, despite being a very big number, is absolutely negligible with respect to $2^{\lambda^N} \approx 10^{3000}$, for every reasonable δD. This result quantitatively explains why almost every random imaginable configuration of (black/white) pixels will not look fractal. In other words, the whole universe of patterns is comparatively really small. This fact may have important applications in Pattern Recognition Theory, e.g. for sizing some hypothetical storage of images (or even texts, etc.), if it was possible to know in advance, that they are (or are composed of) patterns and not just a mere set of pixels (or letters, etc.).

[3] Intuitively, one will arrive to the same conclusion by just observing that $\bar{\Omega}(D) \sim \Omega(D)^{(\bar{\lambda}/\lambda)^N}$.

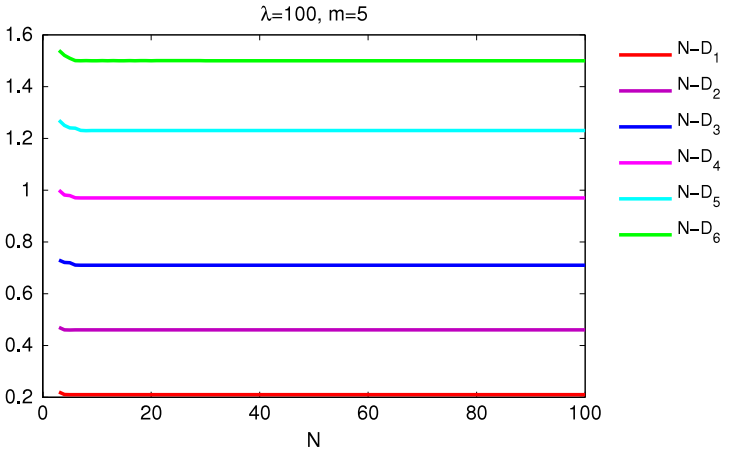

Fig. 4. Dependence of D_i ($i = 1, \ldots, 6$) on N ($\lambda = 100$). Note that $D_i - D_{i+1} \approx const. = 0.237$, independently of N and i.

4.2

Eq. (19) is clearly a self-similar relation (multiplication by a constant). A similar case occurs between every pair (S_{N_1}, S_{N_2}) of entropy functions, associated to different embedding dimensions (N_1, N_2). In general, from Eq. (18), it is easy to check that the shape of $S(D)$ approximately depends only on the difference $N - D$. Then, for $D \geq 3$ (and reasonable m):

$$S_{N_1}(D) \approx \lambda^{-N_2+N_1} S_{N_2}(D + N_2 - N_1) \tag{22}$$

meaning that the entropy functions S_{N_1} and S_{N_2} are related via a translation in D and a multiplication by a constant, clearly a self-similar relationship again. The most important lesson that we can learn from this is that the shape of $S(D)$ is *virtually independent of the dimensionality* N. This opens the doors to a convenient characterization of the components of the system, by means of the values D_i satisfying

$$\frac{d^i S(D = D_i)}{\mathrm{d}D^i} = 0, \quad i = 0, 1, 2, \ldots. \tag{23}$$

Indeed, while $S(D_0) = 0$ for

$$D_0 \approx N, \tag{24}$$

D_1 provides the location of the maximum of the generalized entropy, D_2 is associated with the dimension at which entropy reaches its maximum growth rate, etc. Note that according to Eq. (19), the points D_i have a robust definition in terms of λ. The location of the points D_i is, in a very good approximation, evenly spaced (see Fig. 4), independently of the embedding dimension N. This can be seen as a consequence of another self-similar relation, now shared by $S(D)$ and its derivative:

$$S'(D) \approx AS(D + b), \tag{25}$$

where A and b minimize the quadratic norm of the difference of both members over the range $0 \leq D \leq N - b$, as Fig. 5 shows.[4] From the figure, it can be observed that the self-similarity is very accurate. Clearly, by differentiating iteratively Eq. (25), one has that the points D_i satisfy:

$$D_i - D_{i+1} \approx b, \quad i = 0, 1, 2, \ldots \tag{26}$$

(see Fig. 4).

In the fractal system of Ref. [13], embedded in the spatial dimension $N = 2$, the authors have associated the zeros D_i of the derivatives of $S(D)$, with the edges of different classes or types of urban layouts, exhibiting different levels of risk regarding urban expansion, thus requiring different planning actions from expert policy-makers.[5] In the fractal system of Ref. [17], equivalent ideas were applied for controlling deforested areas in the Amazon.

Now, let us think about a given cell. Let us imagine we only know that its fractal dimension D follows a random evolution that is approximately increasing in time. Actually, for cancerous tissues, deforested areas and built-up areas (etc.), this is a reasonable assumption because all of them evolve by increasing their sizes (volumes), becoming more and more compact and, consequently, can be considered as having approximately increasing local fractal dimensions (see e.g. Refs. [13,17]).

[4] An analytical explanation of this, can be found in Appendix C.

[5] One can check that the D_i proposed in that paper are approximately evenly spaced as Eq. (26) predicts, though this fact was not explained there.

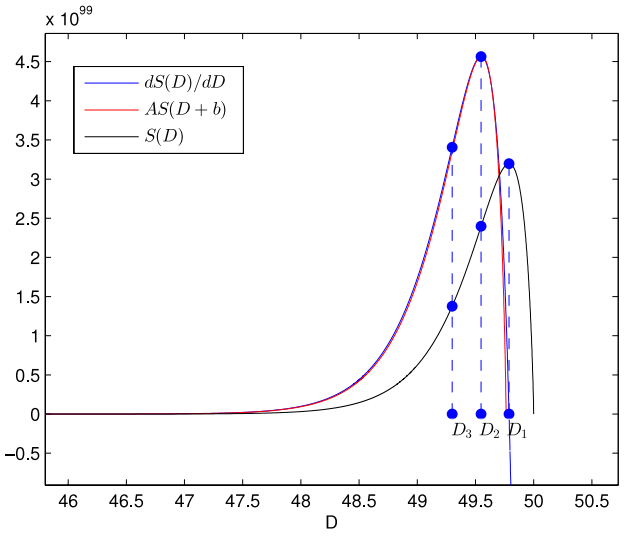

Fig. 5. Qualitative self-similarity shared between $S(D)$ and its derivative ($N = 50$, $\lambda = 100$). Numerically, it turns out that $A = 1.430$ and $b = 0.237$. D_1, D_2 and D_3 are the zeros of the first three derivatives of $S(D)$ and approximately satisfy Eq. (26).

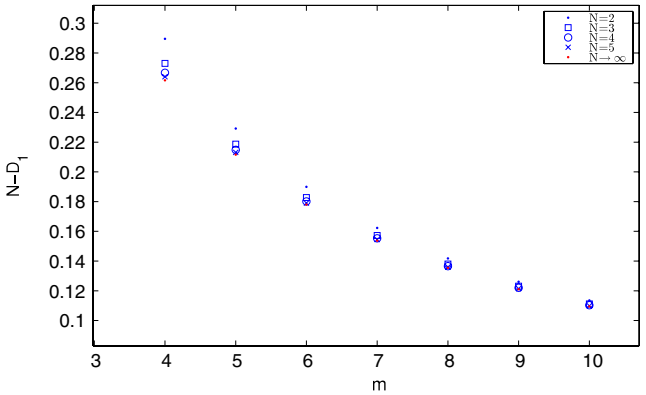

Fig. 6. Plot of $N - D_1$ for many possible *BCM* steps m and dimensionality N. According to Eqs. (24) and (26), $N - D_1 \approx b$ which goes as m^{-1} (see Eq. (C.5)).

Within the range $D < D_1$, $S(D)$ is an increasing monotonous function so, every time D gets higher, we know less about what is going on inside the cell than before. The opposite occurs for $D > D_1$: just increasing D a bit makes the number of possible configurations $\Omega(D)$ to decrease several orders of magnitude (see Figs. 2 and 5), meaning that the cell becomes more and more predictable. Actually, $[D_1, N]$ is a short interval of length decreasing as m^{-1} (see Fig. 6), i.e. an abyss through which $\Omega(D)$ usually decays thousands of orders of magnitude (see Eq. (10)), until reaching the almost absolutely predictable state at $D = N$ ($S(N) \approx 0$, see Eq. (18)). This classification can be enhanced by taking into account D_2. For $D < D_2$, the rate of change of $S(D)$ increases, which means that not only our ignorance is rising but, it also does it every time faster. The opposite happens for $D > D_2$ in which, despite $\mathrm{d}S(D)/\mathrm{d}D$ decreases, there isn't so much that we can do in order to control the cell because first, our ignorance $S(D)$ about its dynamics will go through a range in which it is maximized (i.e. say $D_2 < D < \hat{D}_2 < N$, with $S(\hat{D}_2) = S(D_2)$), going later ($D > \hat{D}_2$) into the increasingly predictable (good or bad) regime mentioned above. Thus, D_2 may define a theoretical limit for steering the component before the things go wrong, as it is concluded both in Refs. [13, 17]. Actually, $[D_3, D_2]$ may be the unique problematic interval in which the chances of controlling the system are still not low because, the range $D < D_3$ can be seen as a regime of low entropy being – perhaps – highly controllable.[6] Of course, it is possible to continue classifying further regimes by also taking into account D_4, D_5, etc., developing a classification that will be consistent with the different regimes found in the entropy and independent of the observer's point of view.

[6] The analogy with cancerous processes is remarkable: $[D_3, D_2]$ may be associated with the stage of having microscopic clusters of cancer cells inside a living tissue, when usually the odds of saving the patient are still not low; while $[D_2, D_1]$ represents a regime in which there are (sometimes macroscopic) metastatic chunks of cancerous tissue that almost no treatment can stop.

5. Entropically driven systems

Section 2.1 introduced the concept of *ideal worst possible scenario*, which was represented by the state ρ_* defined in Eq. (1). Now, with the help of the ideas and mathematics developed in the previous sections, we shall study general properties associated to systems evolving in time towards ρ_*, which we will call from now on, *entropically driven systems*.

Sciences often attempt to define ideal situations but, as it was commented in Section 2.1, in the case of complex control systems it may be very helpful to set the point of reference at the worst ideal situation because, roughly speaking, this kind of systems almost always tends to behave as we don't want.[7]

Given that entropy is a measure of ignorance/uncertainty, and assuming that what cannot be controlled is precisely what is ignored, $S(D)$ may provide a way to assess how much out-of-control the cells having dimension D can be. By analogy to Newton's concept that *a body can ideally move at a constant velocity through a non-friction media*, the *friction* for the complex systems studied here may be represented by every possible constraint, that keeps the system apart from its natural most uncontrolled state, in which the number of components of each type is determined by its maximum degree of uncontrollability. Thus, Eq. (1) may be seen as a metastable state, resulting from a hypothetical evolution *in the absence of control* (fields/constraints of any kind). In addition, this state may also be recognized as a self-organized one, because ρ_* is a non-uniform density and it is assumed that the system can reach it, being – purely – driven by its own entropy.

5.1

It is remarkable that independently of N, if the system distribution is given by ρ_*, the intervals $[D_3, D_1]$ and $[N-1, N]$ will approximately incorporate more than 50% and 76% of the cells, respectively (see Figs. F.8 and F.10). Consequently and specially for large N, an entropical evolution of the system could ultimately imply a potential lack of robustness and fault-tolerance, in the sense that some external force could affect a big part of the system, despite acting on the components of a narrow interval of patterns.

Even worse, according to the patterns' classification developed in Section 4.2, which is independent of the density distribution, ρ_* will have half of its total population lying at the problematic interval $[D_3, D_1]$, and a bit more than this will be lying beyond the theoretical steering limit D_2 (Fig. F.9). Thus, controlling a system like this may be a very difficult task. Clearly, this reinforces the idea of the worst possible scenario associated to ρ_*.

On the other hand, it is noteworthy that the rate of growth, as a function of N, of the number of possible configurations is by far faster than exponential (see Eq. (10)). This means that every time that the embedding dimension increases, the diversity of configurations for fixed D will increase significantly. Thus, assuming that the density of the system ρ had reached a self-organized equilibrium mimicking ρ_* – which is not necessarily the case – and, if it was possible to lessen the inherent constraints associated with the embedding dimension, by increasing the dimensionality from N to $N+\Delta N$, it could let the components of the system evolve following higher dimensional patterns, opening the possibility for significant diversification. Furthermore, in some cases, even under an entropical evolution, the new equilibrium given by $S_{N+\Delta N}(D)$ will initially act to increase the variance σ^2 of the patterns, improving the robustness of the system, in the sense mentioned above.[8]

In addition, because of Eq. (22), every D_i will be shifted by ΔN. This means that every component lying initially beyond the steering limit point D_2 (Section 4.2), will automatically lie on the left of the new D_2 (associated to $S_{N+\Delta N}(D)$), becoming more controllable, in principle. This suggests that, if it was possible to increment the dimensionality by ΔN – whatever be the way this could be done –, it should not be imagined as the mere fact of (e.g.) taking into account a geometrical axis that had been neglected – for simplicity – while one was modeling the system, but as a huge expansion of the space of configurations into which every component of the system is now able to go (and not before), together with a notable improvement in the system's controllability.[9]

However, since the system is entropically driven, the ultimate state will be determined by $S_{N+\Delta N}(D)$, so it will lack robustness and controllability in the same way as the initial state (Eqs. (1) and (22)). Thus, in the absence of control and – as a metaphor of what is observed in many complex control systems –, the hypothetical improvements both in robustness and controllability mentioned above are not something that will last forever, so the system will tend to be out-of-control again.

5.2

I conclude by providing some suggestions of problems and systems for which I believe it could be possible to create concrete applications from the general ideas developed here; besides, the issue of how increasing complexity may evolve in this realm is addressed.

Let us consider a given cell of the multi-component system having fractal dimension D. *Per se*, the hyper-pixels of the cell encode all the information about this particular part of the system. This encoding is what we may designate as *strategy* in the

[7] I.e., the complex control systems that behave as we already want are not usually recognized as problematic.

[8] This will be the case e.g., if the variation of σ^2 occurs mainly in the direction of the normalized $S_{N+\Delta N}(D)$ (see Appendix E).

[9] Note that this idea still may work for $\Delta N < 1$ (whatever that means) because ρ_* is concentrated for high dimensions.

sense that it may describe a kind of pattern of behavior of the part (or agent) belonging to the system associated to the cell (sometimes, it could be related to a way to accomplish some goal). For instance, in urban planning [13], each strategy encodes a specific pattern of urban layout and land use. In other words, we may associate a given (interval of) fractal dimension(s) D to each strategy. If we assume a population of individuals, then different individuals may adopt diverse varieties of a given strategy, that is, different sequences of hyper-pixels leading to the same D. As I have demonstrated here, there is a number of configurations accessible to each D, which is given by $S(D)$ and it is constrained by $L(D)$ and $U(D)$. Furthermore it is clear that, at least in some systems[10] and in the absence of control, the systems will evolve in time in such a way that the population density of strategies $\rho(D)$ will tend to mimic the normalized $S(D)$. Given the behavior of $S(D)$ mentioned above, this means that the majority of the population will employ strategies lying in a short interval of high dimensions, which corresponds to a lack of diversity in the number of strategies used, as well as with a low degree of system controllability.

If we think in terms of economics, this means that the natural tendency countrywide will be to specialize in connection with a narrow set of activities (say, related to *farming* and/or *textile*, or to *oil production*). In the context of international commerce, this may reflect a tendency for the majority of the commercial actors to find partners or allies in the same area of the world. This, in turn, may be undesirable, and governments and/or agencies may implement policies which constitute the necessary *external field* to ensure that the systems remain "*far from equilibrium*", with an associated $\rho(D)$ significantly more uniform than $S(D)$ (that is, diversifying the systems portfolio [21]), being it by fostering the increase of "*production means*", being it by increasing the number of "*partners*", so as to improve systems robustness, fault-tolerance and controllability. It is also worth mentioning that by increasing the dimensionality of a (hierarchical) system from N to $N + \Delta N$, one not only increases its inherent complexity but, given the rise of a new available set of strategies, it also paves the way for a potential diversification. This may be related to the open problem of understanding the major transitions in evolution [22].

All these last ideas are not the main issue of this article but, naturally, they could be the topic of future research.

6. Conclusion

Despite the N-dimensional generalization of $S(D)$ originally defined in Ref. [13] is straightforward, neither clear nor explicit formula for this function had been known until now. Thus, Eq. (18) enabled us both to compute it numerically for higher dimensional systems, and to discover many self-similar relations this quantity satisfies. All these manifestations of self-similarity are the foundation of the general framework for representing complex systems introduced in this article, which provides a quantitative way to classify the components of the system according to its degree of uncontrollability (given by the function $S(D)$), that is independent of the observer's point of view (Section 4). For many complex systems, setting our point of reference at the state distribution ρ_* may also help to assess[11] how far is the system from becoming out-of-control, an aspect that many times it seems hard to be unraveled, mainly when these scenarios represent emergent phenomena.[12]

This work neither points out which part of a given real complex control system can be modeled as one having local fractal dimensions, nor indicates the way to define the N-dimensional space in which it is embedded.[13] Even so, hierarchical systems are ubiquitous in the natural world and, given that the hypothesis on the basis of the ideas studied here are so general, it is likely that the multi-component systems we were dealing with may comprise a non-negligible fraction of the hierarchical systems observed, and to which the principles discussed here do apply.

Acknowledgments

This research was initially supported by the grant SFRH/BPD/63765/2009 provided by FCT Portugal. I want to thank Prof. J.M. Pacheco, who made my ideas flourish and develop extensively, as well as the rest of the members of ATP-group (U. of Lisbon) for their helpful discussions. I would like to thank S. Encarnação because without her precious data, I would have never thought about writing this article.

Appendix A. Number of configurations for fixed V and D

The function $f(x, y, z)$ used in Eq. (5) corresponds to finding out the number of ways of setting z balls into y boxes with x compartments, leaving at least 1 ball per box. This is given by [13]:

$$f(x, y, z) = \binom{xy}{z} p, \tag{A.1}$$

10 These will be systems to which the concept of energy does not apply in a strict sense, in such a way that system's evolution is purely entropical.

11 E.g., by computing $\|\rho - \rho_*\|$, for a given norm $\|\cdot\|$.

12 From some point of view, ρ_* may contribute to know a bit about the unknown but knowable part of the complex system dynamics [23].

13 Although, in hindsight, the models of Refs. [13,17], besides providing a proof of principle of how this formulation can be applied to real cases, also offer some clues of how to address multi-component systems from this perspective.

where $0 \leq p \leq 1$ and it is given by $p =_x F_{x-1}(u; v; 1)$, being F a generalized hypergeometric function, and u and v vectors defined by:

$$u_j = \frac{z-1+j}{x} - y, \quad j = 1, \ldots, x,$$

$$v_j = \frac{j}{x} - y, \quad j = 1, \ldots, x-1.$$

This leads to a closed formula for the total number of configurations Ω with fixed V and D [13]:

$$\Omega(V, D) = \prod_{k=1}^{m} f(2^N, V/2^{kD}, 2^D V/2^{kD}) \tag{A.2}$$

$$= \prod_{k=1}^{m} \binom{2^N V/2^{kD}}{2^D V/2^{kD}}_{2^N} F_{2^N-1}(u; v; 1) \tag{A.3}$$

where

$$u_j = V\frac{2^{D-N}-1}{2^{kD}} + \frac{j-1}{2^N}, \quad j = 1, \ldots, 2^N,$$

$$v_j = \frac{j}{2^N} - \frac{V}{2^{kD}}, \quad j = 1, \ldots, 2^N - 1. \tag{A.4}$$

Appendix B. Some estimates and properties of $f(x, y, z)$

B.1. $f(x, ty, tz)$ is an increasing function of t

Clearly, the number of ways of arranging tz balls into ty boxes (with x compartments), leaving non-empty boxes, cannot be less than the number of ways obtained by doing it leaving z balls every y boxes. Thus, $f(x, ty, tz) \geq f(x, y, z)^t$ so,

$$f(x, ty, tz) \geq f(x, y, z). \tag{B.1}$$

B.2. $\log f(x, y, z) \approx \log\binom{xy}{z}$ for y and z being large numbers

Let us take advantage of the alternative formula for f introduced in Ref. [13]

$$f(x, y, z) = \sum_{k=0}^{[y-z/x]} (-1)^k \binom{y}{k} \binom{x(y-k)}{z} \tag{B.2}$$

and valid for $y \leq z \leq xy$. Without loss of generality, we can assume that $K \doteq y - z/x$ is integer, even and greater than 3. Then, the above equation can be written as follows:

$$f(x, y, z) = g(K/2) + \sum_{r=0}^{K/2-1} (g(r) - g(r+1/2)) \tag{B.3}$$

where $g(r) = \binom{y}{2r}\binom{x(y-2r)}{z}$. The second summand of the right member of (B.3) can be seen as a Riemann's sum for $-dg(r)/dr$; thus, it follows that:

$$f(x, y, z) \approx \frac{g(K/2) + g(0)}{2} = \frac{1}{2}\left(\binom{xy}{z} + \binom{y}{z/x}\right). \tag{B.4}$$

By taking into account that $\binom{xy}{z} \geq \binom{y}{z/x}^x$ and the fact that $x = 2^N > 1$, it is possible to neglect the 2nd summand of the last equation, provided that we take logarithm of both members:

$$\log f(x, y, z) \approx \log\binom{xy}{z} - 1. \tag{B.5}$$

Finally, given that y and z are usually large numbers, $\log\binom{xy}{z} \gg 1$, getting to Eq. (8).

Appendix C. Self-similarity between $S(D)$ and its derivative

According to Eqs. (16) and (17), one has that

$$S(D) \approx U 2^N H(2^{D-N}) \sum_{k=1}^{m} 2^{-kD}. \tag{C.1}$$

Now, because of Eqs. (4) and (14), for $h \to 0$ we have:

$$\begin{aligned} S(D+h) &\approx \log \Omega(2^{mh}U, D+h) \\ &\approx 2^{mh} \log \Omega(U, D+h) \quad \text{because of Eq. (C.1)} \\ &\approx 2^{mh}\left(S(D) + \frac{\Omega_D(U,D)}{\Omega(U,D)\ln 2}h + O(h^2)\right). \end{aligned} \tag{C.2}$$

By taking away $S(D)$ and dividing by h, one has that

$$S'(D) = S(D)m\ln 2 + \frac{\Omega_D(U,D)}{\Omega(U,D)\ln 2}. \tag{C.3}$$

Thus, from the last two equations:

$$2^{-mh}S(D+h) - hS'(D) \approx (1 - hm\ln 2)S(D) + O(h^2). \tag{C.4}$$

Given that the above equation holds for a range of h, this parameter can be chosen in order to minimize the quadratic norm of both members by taking $h = (m\ln 2)^{-1}$. In this way, h will be even decreasing with the number of steps m of the *BCM*, so we can neglect 2nd order terms $O(h^2)$ to arrive at the desired self-similar Eq. (25), whose parameters A and b can be estimated as:

$$\begin{aligned} b &\approx \frac{1}{m\ln 2} \\ A &\approx \frac{m\ln 2}{e}. \end{aligned} \tag{C.5}$$

Despite the above two equations are just estimates, they show a reasonable correspondence with the optimal ones (see e.g. Fig. 5). Even the estimate of b follows the m^{-1} behavior mentioned at Fig. 6 and it is independent of the dimensionality N, as it can be concluded from Eq. (26) and Fig. 4.

Appendix D. Coarse-graining level λ

Many real world fractal systems should not be recognized as having just a single fractal dimension. Think about a chunk of cancerous tissue, the built-up area of a big city or deforested areas in the Amazon. Several authors have associated *whole* fractal dimensions to them but, at the same time, this kind of systems sometimes also present spatial dependence in the fractal dimension, because they are, in part, randomly generated. Clearly, they will be better represented by assigning local fractal dimensions to their components. On the other hand, the diversity of the fractal dimensions of the components is very important; otherwise, we will always be satisfied with the knowledge of a single fractal dimension associated with the whole system, ignoring what happens at every particular part of it.[14] Thus, it will be assumed that the systems of the present article can be decomposed into parts having (maybe) different fractal dimensions. However, if the size of these parts are very small, the fractal behavior could simply vanish or get not properly represented.[15] Is there any way to choose an optimal coarse-graining level so as to simultaneously maximize both the diversity in dimensions and the quality of how they are defined? This was already done in Ref. [13]. Here, I extend the idea to higher dimensional systems and justify, even better than before, why the idea should work for a non-negligible part of the total universe of fractal complex systems.

Let us assume that the system is discretized in hyper-pixels (of side equal to 1), and that it fits inside of a hyper-cube of side Δ (in pixels) in a space of dimensionality N. The pixels (not) belonging to the system will be black (white). Let us divide the whole system into cells of side λ, i.e. the coarse graining level. If λ is chosen to be equal to Δ, the *BCM* will return a number D, and we call it *the fractal dimension of the whole system* (see Fig. D.7). If one divides the system into cells of side $\lambda = \Delta/2$, the *BCM* will return at most 2^N fractal dimensions, i.e. one – maybe different – fractal dimension per cell.[16] Thus, if our spatial resolution is good (i.e. if the size of the pixels is small enough), the number of fractal dimensions spanned by performing the *BCM* at each cell, will increase by reducing the size of the cells but, at the same time, will always remain bounded by $N/\delta D$ (where δD is the precision of the computation of the fractal dimensions). On the other hand, because of finite size effects, if the size of the cells is very small, not only the fractal behavior will vanish, but also the total number of black/white pixels configurations of a cell will decrease significantly and, consequently, the fractal configurations will do so [one can roughly think that at the limit $\lambda \to 1$, one will only get two fractal dimensions: $D = 0 (D = N)$ for the cells consisting of a single white (black) pixel]. Between $\lambda = 1$ and $\lambda = \Delta$, it is reasonable to assume the existence of some set of coarse-graining levels Γ in which the number of fractal dimensions spanned by the *BCM* is maximized (for the precision δD). In addition, the larger the value of λ, the larger the number of steps m of the performed *BCM*, resulting the fractal dimension

14 The diversity of the components is an important idea that every model for complex systems should incorporate [23].

15 E.g., if the fractal dimension of a cell of black/white pixels is given by the slope of the linear fitting of the Box-counting-method.

16 It is important to remember that the fractal systems studied in this work are in part randomly generated.

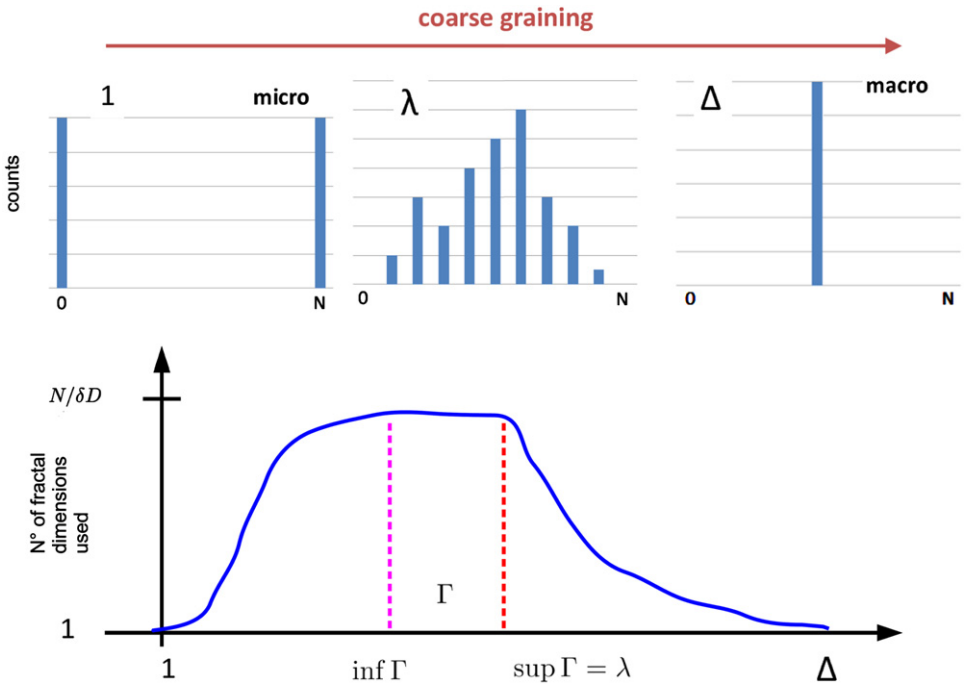

Fig. D.7. Top: The different panels illustrate the diversity in fractal dimensions exhibited by the same N-dimensional, hierarchical system, depending on the level of coarse-graining at which the fractal analysis is carried out. Bottom: The same idea, in terms of the number of fractal dimensions used (for a given precision δD). It is possible to assume the existence of an intermediate level λ at which fractal information is optimal.

at every cell to be shared at a larger number of scales and naturally, more properly defined (Eqs. (2) *and* (3)). Thus, we define *the optimal coarse-graining level* λ $(1 < \lambda < \Delta)$ as follows:

$$\lambda \doteq \sup \Gamma, \tag{D.1}$$

providing an optimal portrait of the fractal behavior of the system (see Fig. D.7).

Finally, it is worth remarking that just for the sake of being precise, it is proposed to use Eq. (D.1) but fortunately, it is not necessary to know the exact value of λ, because all the ideas of this article are robust to the choice of it, as it is concluded at Eq. (19).

Appendix E. $S_{N+\Delta N}$ initially acts to increase the variance of D

Lemma. *Let us denote by* ρ_{*N} *and* $\rho_{*N+\Delta N}$ *the densities defined by Eq.* (1) *associated to embedding spaces of dimensionality* N *and* $N + \Delta N$*, respectively. Let us suppose that the initial cell distribution is given by*

$$\rho_0(D) = \begin{cases} \rho_{*N}(D) & 0 \le D \le N, \\ 0 & N < D \le N + \Delta N. \end{cases} \tag{E.1}$$

Then, in the direction of $\rho_{*N+\Delta N}$*, the variance of the fractal dimension will initially increase.*

Proof. The variance σ^2 can be seen as a function of the state ρ:

$$\sigma^2(\rho) = \int_0^{N+\Delta N} D^2 \rho(D)\, \mathrm{d}D - \left(\int_0^{N+\Delta N} D\rho(D)\, \mathrm{d}D \right)^2. \tag{E.2}$$

The following track makes to increase ρ_0 in the direction of $\rho_{*N+\Delta N}$:

$$\rho_t = \rho_0 + t(\rho_{*N+\Delta N} - \rho_0) \quad 0 \le t \le 1 \tag{E.3}$$

(note that $\rho_t(D) \ge 0$ and $\int_0^{N+\Delta N} \rho_t(D)\, \mathrm{d}D = 1$). Then, one can replace Eq. (E.3) in Eq. (E.2), differentiate it twice with respect to t and obtain:

$$\begin{aligned} \frac{d^2\sigma^2(\rho_t)}{\mathrm{d}t^2} &= -2 \left(\int_0^{N+\Delta N} D(\rho_{*N+\Delta N}(D) - \rho_0(D))\, \mathrm{d}D \right)^2 \\ &\approx -2(\Delta N)^2 = const. \end{aligned} \tag{E.4}$$

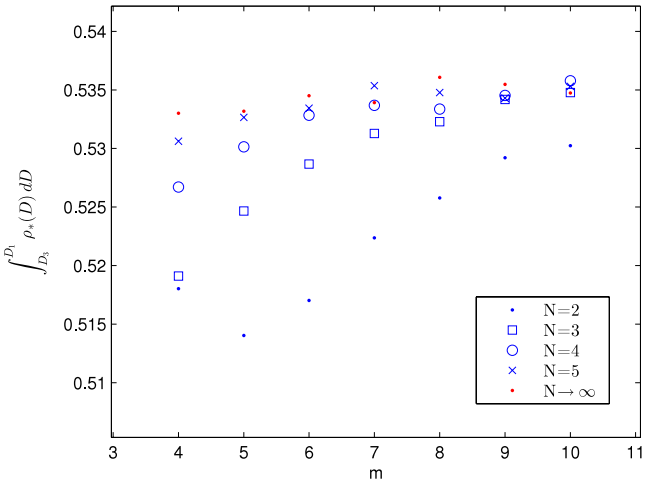

Fig. F.8. Independently of N and m, more than 50% of the individuals will lie within the zeros of the 3rd (D_3) and the 1st (D_1) derivatives if they follow the distribution ρ_*.

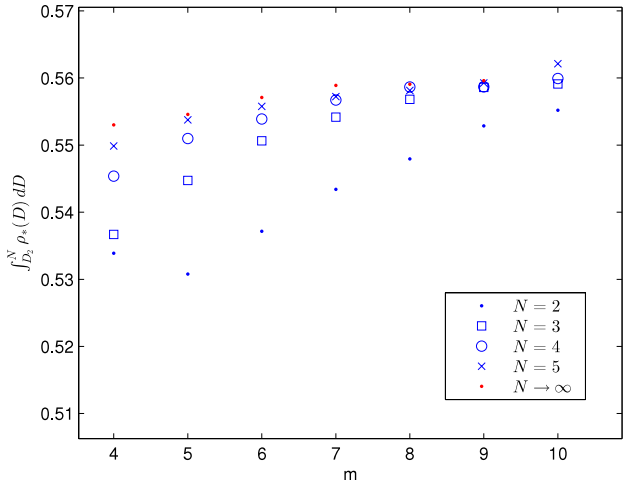

Fig. F.9. Independently of N and m, more than 53% of the individuals will lie within the range $D_2 \leq D \leq N$, if they follow the distribution ρ_*.

because of Eq. (22). Eq. (22) also says that the standard deviations at $t = 0$ and at $t = 1$ will be approximately equal. Thus, for the track of Eq. (E.3), the variance reads:

$$\sigma^2(\rho_t) \approx \sigma^2(\rho_0) + t(1-t)(\Delta N)^2. \tag{E.5}$$

Then,

$$\left(\frac{d\sigma^2(\rho_t)}{\mathrm{d}t}\right)_{t=0} \approx (\Delta N)^2 > 0. \quad \square \tag{E.6}$$

Eq. (E.5) gives the variance along a path connecting ρ_{*N} and $\rho_{*N+\Delta N}$ (Eq. (E.3)), which has a maximum value of $\sigma^2(\rho_o) + (\Delta N)^2/4$. Note that for this hypothetical track, the variance cannot increase indefinitely and it will necessarily go back to its initial value, sooner or later, because the system is entropically-driven. Besides, this track is by no means the unique one that makes the variance to increase (initially). Actually, Eq. (E.2) can be considered as a continuous map $\rho \to \sigma^2(\rho)$.[17] This means that, if ΔN is not excessively small, at least there will exist a positively measurable set of tracks, with initial increasing variances.

[17] This will be the case e.g., if one considers that the tracks are differentiable functions of t, the norm of every path ρ_t is given by $\max_t(\max_D |\rho_t(D)| + \max_D |\partial\rho_t(D)/\partial t|)$ and, the norm of every σ_t^2 is defined as $\max_t |\sigma_t^2| + \max_t |d\sigma_t^2/\mathrm{d}t|$.

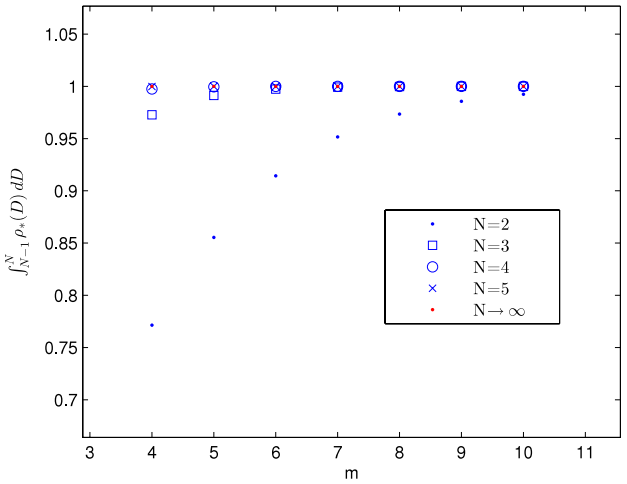

Fig. F.10. Independently of N and m, more than 76% of the individuals will lie within the range $N - 1 \leq D \leq N$ (and more than 95% for $N > 2$), if they follow the distribution ρ_*.

Appendix F. $\rho_*(D)$ is concentrated for high dimensions

See Figs. F.8–F.10.

References

[1] P.W. Anderson, More is different, Science 177 (1972) 393.
[2] E. Ravasz, A.L. Barabási, Hierarchical organization in complex networks, Phys. Rev. E 67 (2003) 026112.
[3] R. Albert, A.L. Barabási, Statistical mechanics of complex networks, Rev. Modern Phys. 74 (2002) 47–97.
[4] R.G. Palmer, D.L. Stein, E. Abrahams, P.W. Anderson, Models of hierarchically constrained dynamics for glassy relaxation, Phys. Rev. Lett. 53 (1984) 958.
[5] L.D. Carlos, J.M. Pacheco, R.A.S. Ferreira, A.L.L. Videira, Hierarchically constrained dynamics and emergence of complex behavior in nanohybrids, Small 6 (2010) 386–390.
[6] B. Mandelbrot, The Fractal Geometry of Nature, Macmillan, 1983.
[7] E. Stanley, P. Meakin, Multifractal phenomena in physics and chemistry, Nature 335 (1988) 405–409.
[8] B. Mandelbrot, Multifractal measures, especially for geophysicist, Pure Appl. Geophys. 131 (1-2) (1989) 5–42.
[9] R. Lopes, N. Betrouni, Fractal and multifractal analysis: A review, Medi. Image Anal. 13 (2009) 634–649.
[10] F. Schimitt, D. Schertzer, S. Lovejoy, Multifractal analysis of foreign exchange data, Appl. Stoch. Models Data Anal. 15 (1999) 29–53.
[11] S. Sabanal, M. Nakagawa, The fractal properties of vocal sounds and their application in the speech recognition model, Chaos Solitons Fractals 7 (11) (1996) 1825–1843.
[12] A. Rodriguez, L.J. Vasquez, K. Slevin, R.A. Römer, Multifractal finite-size-scaling and universality at the anderson transition, Phys. Rev. B 84 (2011) 134209-16.
[13] S. Encarnação, M. Gaudiano, F.C. Santos, J.A. Tenedório, J.M. Pacheco, Fractal cartography of urban areas, Sci. Rep. 2 (2012) 527. http://dx.doi.org/10.1038/srep00527.
[14] H. Simon, The architecture of complexity, Proc. Am. Phil. Soc. 106 (6) (1962) 467–482.
[15] J. Doyle, Computational biology: Beyond the spherical cow, Nature 411 (2001) 151–152.
[16] Sara Encarnação, Espaço geográfico e complexidade: modelação do crescimento das áreas construídas na aglomeração de Lisboa (doctoral thesis in Geography), FCSH, U. Nova de Lisboa, 2011, (in portuguese) http://hdl.handle.net/10362/7206.
[17] J. Sun, Z. Huang, Q. Zhen, J. Southworth, S. Perz, Fractally deforested landscape: Pattern and process in a tri-national Amazon frontier, Appl. Geogr. 52 (2014) 204–211.
[18] J.W. Baish, R.K. Jain, Fractals and cancer, Cancer Res. 60 (2000) 3683–3688.
[19] K.J. Falconer, Fractal Geometry: Mathematical Foundations and Applications, John Wiley & Sons Inc., 2003.
[20] S.Y. Auyang, Foundations of Complex-System Theories, Cambridge Univ. Press, 1998.
[21] W.C. Kim, R. Mauborgne, Blue Ocean Strategy, Harvard Bussiness School Press, 2005.
[22] John M. Smith, Eörs Szathmáry, The Major Transitions in Evolution, Oxford University Press, 1995.
[23] S. Levin, Complex adaptive systems: Exploring the known, the unknown and the unknowable, Bull. Amer. Math. Soc. (N.S.) 40 (1) (2002) 3–19.